Inorg. Chem. **2007**, *46*, 5174–5178

Synthesis, Structure, and Luminescent and Magnetic Properties of Novel Lanthanide Metal–Organic Frameworks with Zeolite-like Topology

Zhongyue Li, Guangshan Zhu,* Xiaodan Guo, Xiaojun Zhao, Zhao Jin, and Shilun Qiu*

State Key Laboratory of Inorganic Synthesis & Preparative Chemistry, Jilin University, Changchun 130012, China

Received September 3, 2006

A series of microporous lanthanide metal–organic frameworks [Ln(BTC)(DMF)$_2$·H$_2$O, Ln = Tb (**1**), Dy (**2**), Ho (**3**), Er (**4**), Tm (**5**), Yb (**6**); DMF = *N*,*N*′-dimethylformamide] with 4·4·4·6·6·8 topology, which is very common in the zeolite topologies, have been synthesized under mild conditions. The single-crystal X-ray diffraction analysis reveals that they exhibit the same three-dimensional (3D) architecture and crystallize in monoclinic symmetry space group *C*2/*c*. Organic and inorganic four-connected nodes link each other to form a 3D open framework. The framework contains approximate 13 Å × 7 Å rectangle channels along the [1,1,0] and [1,–1,0] directions, respectively. The luminescent properties of these complexes have been studied, and complex **1** shows a Tb^{3+} characteristic emission in the range of 450–650 nm at room temperature. Complexes **1**–**5** exhibit antiferromagnetic interaction between Ln^{3+} ions. The water sorption isotherm shows that about 15 water molecules per unit cell can be adsorbed into the micropores of dehydrated complex **4**.

Introduction

Expansion and decoration of the topological networks of inorganic materials have been proven as an effective and successful synthetic strategy to synthesizing highly porous metal−organic frameworks (MOFs).[1] Through the replacement of monatomic anions by polyatomic organic ligands as linkers and use of the well-defined coordination geometries of metal centers as nodes, a large number of MOFs with structures of various minerals, especially four-connected nets, such as quartz, diamond, PtS, NbO, $SrAl_2$, and zeolites, have been replicated.[2] Most of the reported MOFs constructed from four-connected nodes are based on transition metals but not lanthanide metals because lanthanide elements are always regarded as unsuitable metal centers, whose coordination numbers are high and coordination geometries are hard to control.[3] However, attracted by the special chemical and physical properties of lanthanide elements, many efforts have been made to synthesize novel lanthanide MOFs.[4] The dissociation or removal of the terminal coordinated molecules from the lanthanide metal centers could make them become Lewis acid sites, which may reveal their potential uses in sensors or as catalysts for organic transformations.[5] According to our preliminary studies, most lanthanide ions of

* To whom correspondence should be addressed: E-mail: zhugs@mail.jlu.edu.cn (G.Z.), sqiu@mail.jlu.edu.cn (S.Q.). Fax: (+86) 431 85168331.

(1) (a) Seo, J. S.; Whang, D.; Lee, H.; Jun, S. I.; Oh, J.; Jeon, Y. J.; Kim, K. *Nature* **2000**, *404*, 982. (b) Chen, B.; Eddaoudi, M.; Hyde, S. T.; O'Keeffe, M.; Yaghi, O. M. *Science* **2001**, *291*, 1021. (c) Sato, O.; Iyoda, T.; Fujishima, A.; Hashimoto, K. *Science* **1996**, *271*, 49. (d) Kahn, O.; Martinez, C. *Science* **1998**, *279*, 44.

(2) (a) Fang, Q. R.; Zhu, G.; Xue, M.; Sun, J. Y.; Wei, Y.; Qiu, S.; Xu, R. *Angew. Chem., Int. Ed.* **2005**, *44*, 2. (b) Tian, Y. Q.; Cai, C. X.; Ji, Y.; You, X. Z.; Peng, S. M.; Lee, G. H. *Angew. Chem., Int. Ed.* **2002**, *41*, 1384. (c) Férey, G.; Serre, C.; Mellot-Draznieks, C.; Millange, F.; Surblé, S.; Dutour, J.; Margiolaki, I. *Angew. Chem.* **2004**, *116*, 6456. (d) Sun, J. Y.; Weng, L. H.; Zhou, Y. M.; Chen, J. X.; Chen, Z. X.; Liu, Z. C.; Zhao, D. Y. *Angew. Chem., Int. Ed*. **2002**, *41*, 4471. (e) Hoskins, B. F.; Robson, R. *J. Am. Chem. Soc.* **1990**, *112*, 1546. (f) Gable, R. W.; Houskins, B. F.; Robson, R. *J. Chem. Soc., Chem. Commun.* **1990**, 762. (g) Chen, B.; Eddaoudi, M.; Reineke, T. M.; Kampf, J. W.; O'Keeffe, M.; Yaghi, O. M. *J. Am. Chem. Soc.* **2000**, *122*, 11559. (h) Eddaoudi, M.; Kim, J.; O'Keeffe, M.; Yaghi, O. M. *J. Am. Chem. Soc.* **2002**, *124*, 376. (i) Rosi, N. L.; Eddaoudi, M.; Kim, J.; O'Keeffe, M.; Yaghi, O. M. *Angew. Chem., Int. Ed*. **2002**, *114*, 294.

(3) (a) Kiritsis, V.; Michaelides, A.; Skoulika, S.; Golhen, S.; Ouahab, L. *Inorg. Chem.* **1998**, *37*, 3407. (b) Long, D. L.; Blake, A. J.; Champness, N. R.; Schroder, M. *Chem. Commun.* **2000**, 1369.

(4) (a) Liu, W. S.; Jiao, T. Q.; Li, Y. Z.; Liu, Q. Z.; Tan, M. Y.; Wang, H.; Wang, L. F. *J. Am. Chem. Soc.* **2004**, *126*, 2280. (b) Ma, B. Q.; Zhang, D. S.; Gao, S.; Jin, T. Z.; Yan, C. H.; Xu, G. X. *Angew. Chem., Int. Ed.* **2002**, *39*, 3644. (c) Serre, C.; Stock, N.; Bein, T.; Férey, G. *Inorg. Chem.* **2004**, *43*, 3159. (d) Mancino, G.; Ferguson, A. J.; Beeby, A.; Long, N. J.; Jones, T. S. *J. Am. Chem. Soc.* **2005**, *127*, 524.

(5) (a) Reineke, T. M.; Eddaoudi, M.; Fehr, M.; Kelley, D.; Yaghi, O. M. *J. Am. Chem. Soc.* **1999**, *121*, 1651. (b) Reineke, T. M.; Eddaoudi, M.; O'Keeffe, M.; Yaghi, O. M. *Angew. Chem., Int. Ed.* **1999**, *38*, 2590. (c) Guo, X. D.; Zhu, G. S.; Li, Z. Y.; Sun, F. X.; Yang, Z. H.; Qiu, S. L. *Chem. Commun.* **2006**, 3172.

10.1021/ic061666i CCC: $37.00
Published on Web 05/19/2007

Table 1. Yields and M_r Values for Complexes **1**−**6**

	yield based on Ln (%)	formula	M_r	anal. calcd	anal. found
1	63	$C_{15}H_{19}TbO_9N_2$	530.25	C, 33.98; H, 3.61; N, 5.28	C, 33.61; H, 3.56; N, 5.20
2	58	$C_{15}H_{19}DyO_9N_2$	533.82	C, 33.75; H, 3.59; N, 5.25	C, 33.02; H, 3.61; N, 5.33
3	52	$C_{15}H_{19}HoO_9N_2$	536.25	C, 33.60; H, 3.57; N, 5.22	C, 33.50; H, 3.42; N, 5.10
4	50	$C_{15}H_{19}ErO_9N_2$	538.58	C, 33.45; H, 3.56; N, 5.20	C, 33.30; H, 3.74; N, 5.12
5	61	$C_{15}H_{19}TmO_9N_2$	540.26	C, 33.35; H, 3.54; N, 5.19	C, 33.30; H, 3.69; N, 5.36
6	53	$C_{15}H_{19}YbO_9N_2$	544.36	C, 33.10; H, 3.52; N, 5.15	C, 33.21; H, 3.59; N, 5.30

coordination polymers have terminal coordinated molecules,[6] which decrease their coordination number linked with organic ligands; therefore, it is not impossible to construct frameworks with four-connected nodes based on lanthanide elements. 1,3,5-Benzenetricarboxylic acid (H_3BTC) has three carboxylic groups with multifarious coordination modes and could be regarded as a good candidate for an organic four-connected node. Some MOFs based on lanthanide and BTC have been constructed successfully.[5c,6c,7] Recently, our group has been engaging in the assembly of novel frameworks with zeolite or zeolite-like topology utilizing transition metals and lanthanide metals. We have succesfully synthesized a novel 3D complex with the zeolite MTN topology with 2522 Å^3 cages via consideration of the hexamethylenetetramine ligand as the organic tetrahedral building block and a series of compounds with ABW topology with 5×8 Å^2 channels based on lanthanide metals and the BTC ligand, and so on.[2a,6c,8] As a sequel, we present herein a series of novel lanthanide MOFs synthesized under mild conditions [$Ln(BTC)(DMF)_2 \cdot H_2O$, Ln = Tb (**1**), Dy (**2**), Ho (**3**), Er (**4**), Tm (**5**), Yb (**6**); constructed from inorganic four-connected nodes (T1, a lanthanide metal ion linked with four phenyl groups through carboxylate groups) and organic four-connected nodes (T2, a phenyl group connected with four metal ions through carboxylate groups). These frameworks contain approximate 13 Å $\times$ 7 Å rectangle channels along the [1,1,0] and [1,−1,0] directions (calculated from the distance of non-hydrogen atom centers), respectively. The luminescent, magnetic, and water adsorption properties of these complexes were investigated.

Experimental Section

All chemicals purchased were of reagent grade or better and were used without further purification. Lanthanide nitrate salts [$Ln(NO_3)_3 \cdot nH_2O$] were prepared via dissolution of lanthanide oxides with HNO_3 (6 M), while adding H_2O_2 for Tb_4O_7. The mixture was then evaporated at 100 °C until a crystal film formed. Fluorescence spectroscopy data were recorded on a LS55 luminescence spectrometer. Temperature-dependent magnetic susceptibility data were obtained on a Quantum Design MPMSXL SQUID magnetometer under an applied field of 1000 Oe over the temperature range of 4−300 K. The elemental analyses were carried out on a Perkin-Elmer 240C elemental analyzer. Thermogravimetric analyses (TGA) were performed under oxygen with a heating rate of 10 °C·min^{-1} using a Perkin-Elmer TGA 7 thermogravimetric analyzer. Powder X-ray diffraction (XRD) data were collected on a Siemens D5005 diffractometer with Cu Kα radiation (λ = 1.5418 Å). The infrared (IR) spectra were recorded (400−4000 cm^{-1} region) on a Nicolet Impact 410 FTIR spectrometer using KBr pellets. Water adsorption measurements were conducted on a CAHN 2000 analyzer at room temperature.

Synthesis of $Tb(BTC)(DMF)_2 \cdot H_2O$ (1). As a typical preparation procedure, a solution of $Tb(NO_3)_3 \cdot nH_2O$ (40 mg, 0.10 mmol), H_3BTC (20 mg, 0.10 mmol), caprolactam (10 mg, 0.10 mmol), DMF (10 mL), and ethanol (2 mL) was stirred for 2 h. Then the above mixture was left at 55 °C for 5 days to give colorless rod crystals.

Synthesis of $Ln(BTC)(DMF)_2 \cdot H_2O$ (2−6). The procedures were the same as that of **1** except that $Tb(NO_3)_3 \cdot nH_2O$ was replaced by the corresponding $Ln(NO_3)_3 \cdot nH_2O$ [Ln = Dy (**2**), Ho (**3**), Er (**4**), Tm (**5**), Yb (**6**)]. The yields and M_r values for **1**−**6** are listed in Table 1.

X-ray Crystallographic Study. The intensity data were collected on a Smart CCD diffractometer with graphite-monochromated Mo Kα (λ = 0.710 73 Å) radiation at room temperature in the $\omega-2\theta$ scan mode. An empirical absorption correction was applied to the data using the *SADABS* program.[9] The structures were solved by direct methods. All non-hydrogen atoms were refined anisotropically. Hydrogen atoms were fixed at calculated positions and refined by using a riding mode. All calculations were performed using the *SHELXTL* program.[10] The crystallographic data are summarized in Table 2, and the selected bond lengths and bond angles of the six complexes are listed in Tables 3 and 4 and Tables S1 and S2 in the Supporting Information.

Results and Discussion

Complexes **1**−**6** have been successfully synthesized under mild conditions. Single-crystal XRD, elemental analysis, IR, and TGA studies performed on the compounds **1**−**6** indicate that they exhibit the same structure with the formula $Ln(BTC)(DMF)_2 \cdot H_2O$ [Ln = Tb (**1**), Dy (**2**), Ho (**3**), Er (**4**), Tm (**5**), Yb (**6**)].

Crystal Structure. These six complexes are isomorphous and isostructural; thus, only the structure of complex **1** is described here in detail. Complex **1** is a 3D open framework, and each asymmetric unit contains one eight-coordinated Tb^{3+} ion, one BTC ligand, two coordianted DMF molecules,

(6) (a) Guo, X. D.; Zhu, G. S.; Fang, Q. R.; Xue, M.; Tian, G.; Sun, J. Y.; Li, X. T.; Qiu, S. L. *Inorg. Chem.* **2005**, *44*, 3850. (b) Guo, X. D.; Zhu, G. S.; Sun, F. X.; Li, Z. Y.; Zhao, X. J.; Li, X. T.; Wang, H. C.; Qiu, S. L. *Inorg. Chem.* **2006**, *45*, 2581. (c) Guo, X. D.; Zhu, G. S.; Li, Z. Y.; Chen, Y.; Li, X. T.; Qiu, S. L. *Inorg. Chem.* **2006**, *45*, 4065.

(7) (a) Rosi, N. L.; Kim, J.; Eddaoudi, M.; Chen, B. L.; O'Keeffe, M.; Yaghi, O. M. *J. Am. Chem. Soc.* **2005**, *127*, 1504. (b) Serre, C.; Millange, F.; Thouvenot, C.; Gardant, N.; Pelle, F.; Férey, G. *J. Mater. Chem.* **2004**, *14*, 1540. (c) Yang, J.; Yue, Q.; Li, G. D.; Cao, J. J.; Li, G. H.; Chen, J. S. *Inorg. Chem.* **2006**, *45*, 2857.

(8) Fang, Q. R.; Zhu, G. S; Xue, M.; Sun, J. Y.; Sun, F. X.; Qiu, S. L. *Inorg. Chem.* **2006**, *45*, 3582.

(9) Sheldrick, G. M. *SADABS, Program for Empirical Absorption Correction for Area Detector Data*; University of Göttingen: Göttingen, Germany, 1996.

(10) Sheldrick, G. M. *SHELXS 97, Program for Crystal Structure Refinement*; University of Göttingen: Göttingen, Germany, 1997.

Table 2. Crystallographic Data for Complexes **1**−**6**

	1	**2**	**3**	**4**	**5**	**6**
empirical formula	$C_{15}H_{19}N_2O_9Tb$	$C_{15}H_{19}N_2O_9Dy$	$C_{15}H_{19}N_2O_9Ho$	$C_{15}H_{19}N_2O_9Er$	$C_{15}H_{19}N_2O_9Tm$	$C_{15}H_{19}N_2O_9Yb$
fw	530.24	533.82	536.25	538.58	540.25	544.36
cryst syst	monoclinic	monoclinic	monoclinic	monoclinic	monoclinic	monoclinic
space group	*C*2/*c*	*C*2/*c*	*C*2/*c*	*C*2/*c*	*C*2/*c*	*C*2/*c*
a (Å)	18.568(3)	18.493(18)	18.440(4)	18.4014(10)	18.382(2)	18.299(4)
b (Å)	11.630(2)	11.580(18)	11.647(2)	11.6492(10)	11.5929(15)	11.592(2)
c (Å)	19.741(4)	19.51(2)	19.698(4)	19.6803(13)	19.632(3)	19.557(4)
β (deg)	107.202(4)	107.22(3)	107.06(3)	106.979(2)	107.086(2)	107.01(3)
V (Å^3)	4072.3(13)	3991(9)	4044.5(14)	4034.8(5)	3998.8(9)	3966.9(14)
Z	8	8	8	8	8	8
T (K)	293(2)	293(2)	293(2)	293(2)	293(2)	293(2)
λ (Å)	0.71073	0.71073	0.71073	0.71073	0.71073	0.71073
ρ_{calc} (g·cm^{-1})	1.730	1.777	1.761	1.773	1.795	1.823
μ (mm^{-1})	3.520	3.792	3.959	4.207	4.485	4.763
R^a [$I > 20\sigma(I)$]	0.0402	0.0494	0.0401	0.0509	0.0593	0.0531
$R_w{}^b$	1.1088	0.1127	0.1104	0.1211	0.1079	0.1429

^{a} $R = \sum||F_o| - |F_c||/\sum|F_o|$. ^{b} $R_w = [\sum w(F_o^2 - F_c^2)/\sum w(F_o^2)^2]^{1/2}$.

Table 3. Selected Bond Lengths (Å) for Complex **1**

Tb1−O6	2.286(5)	Tb1−O1	2.398(6)
Tb1−O5	2.319(5)	Tb1−O3	2.413(6)
Tb1−O7	2.362(6)	Tb1−O4	2.421(6)
Tb1−O8	2.375(6)	Tb1−O2	2.437(5)

Table 4. Selected Bond Angles (deg) for Complex **1**

O6−Tb1−O5	84.43(19)	O1−Tb1−O3	82.5(3)
O6−Tb1−O7	84.0(2)	O6−Tb1−O4	156.6(2)
O5−Tb1−O7	79.2(2)	O5−Tb1−O4	78.5(2)
O6−Tb1−O8	78.8(2)	O7−Tb1−O4	77.2(2)
O5−Tb1−O8	148.6(2)	O8−Tb1−O4	108.1(3)
O7−Tb1−O8	72.8(2)	O1−Tb1−O4	98.3(2)
O6−Tb1−O1	92.8(2)	O3−Tb1−O4	52.98(19)
O5−Tb1−O1	75.62(19)	O6−Tb1−O2	79.04(18)
O7−Tb1−O1	154.8(2)	O5−Tb1−O2	125.15(17)
O8−Tb1−O1	131.2(2)	O7−Tb1−O2	148.1(2)
O6−Tb1−O3	149.64(19)	O8−Tb1−O2	77.51(19)
O5−Tb1−O3	122.7(2)	O1−Tb1−O2	53.72(17)
O7−Tb1−O3	112.3(2)	O3−Tb1−O2	74.04(19)
O8−Tb1−O3	81.8(2)	O4−Tb1−O2	123.95(19)

and one free guest water molecule. Each Tb^{3+} ion is coordinated with eight oxygen atoms from four BTC ligands through two chelating bidentate carboxylate groups (O1−O4), two dimonodentate carboxylate groups (O5 and O6), and two terminal DMF molecules (O7 and O8) (Figure 1). The carboxylic O−Tb bond distances range from 2.286(6) to 2.437(5) Å and the Tb−O_{DMF} distances are between 2.362(6) and 2.375(6) Å, all of which are comparable to those reported for other Tb−O donor complexes.[6,11]

To deeply understand the nature of the involuted frameworks, a topological approach can be used, i.e., reducing multidimensional structures to simple node-and-connection nets. Obviously, in this framework, one Tb^{3+} ion is linked with four phenyl groups through two chelating bidentate carboxylate groups and two dimonodentate carboxylate groups, which could be considered as an inorganic four-connected node (T1; Figure 2a). Likewise, each BTC ligand is connected with four Tb^{3+} ions through carboxylate groups, so it could be regarded as an organic four-connected node (T2; Figure 2b). The vertex symbols of T1 and T2 both are

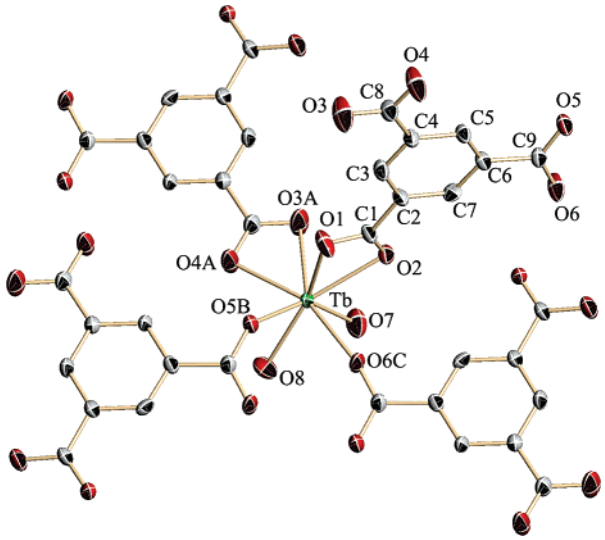

Figure 1. Coordination environment of Tb1 in complex **1** with non-hydrogen atoms represented by thermal ellipsoids drawn at the 30% probability level.

4·4·4·6·6·8, which is very common in zeolite topologies, such as CGS, EAB, ERI, LEV, LTA, and LTL; therefore, it is not unreasonable to regard it as a zeolite-like topology (Figure 2c), though it is not an isostructure with a reported zeolite topology.[12] This framework contains eight-membered rings, which are formed from four metal centers (T1) and four phenyl groups (T2) (Figure 2d). These kinds of eight-membered rings link each other to form approximate 13 Å × 7 Å [Tb (**1**), 13.534 Å × 7.612 Å; Dy (**2**), 13.360 Å × 7.584 Å; Ho (**3**), 13.471 Å × 7.590 Å; Er (**4**), 13.447 Å × 7.581 Å; Tm (**5**), 13.421 Å × 7.584 Å; Yb (**6**), 13.362 Å × 7.578 Å; calculated from the distance of non-hydrogen atom centers] rectangle channels along the [1,1,0] and [1,−1,0] directions, respectively (Figure 2e).

Photoluminescent Properties. It is well-known that the lanthanides, especially europium and terbium, can absorb ultraviolet radiation efficiently through an allowed electronic transition to convert to excited state $^5D_4$, and these excited states are deactivated to the multiplet ^7F_J states radiatively

(11) (a) Wan, Y.; Jin, L.; Wang, K.; Zhang, L.; Zheng, X.; Lu, S. *New J. Chem.* **2002**, *26*, 1590. (b) Liu, C. B.; Sun, C. Y.; Jin, L. P.; Lu, S. Z. *New J. Chem.* **2004**, *28*, 1019. (c) Sun, H. L.; Gao, S.; Ma, B. Q.; Chang, F.; Fu, W. F. *Microporous Mesoporous Mater.* **2004**, *73*, 89.

(12) *Atlas of Zeolite Framework Types*, 5th ed.; Baerlocher, Ch., Meier, W. M., Olson, D. H., Eds.; Elsevier: New York, 2001.

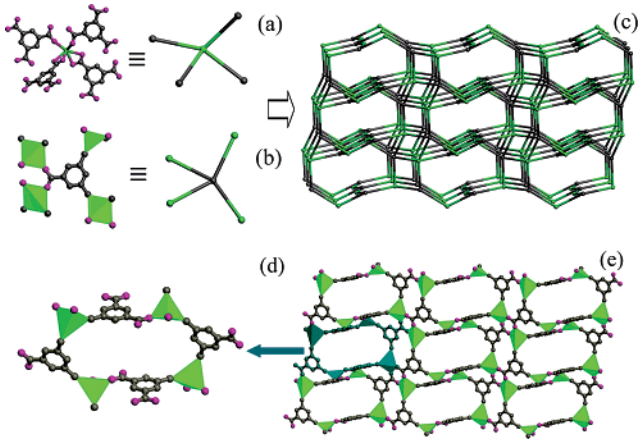

Figure 2. (a) Inorganic four-connected node T1 (Tb^{3+}) of complex **1** coordinated with four phenyl groups (T2) of BTC ligands through two chelating bidentate carboxylate groups and two dimonodentate carboxylate groups. (b) Phenyl group regarded as an organic four-connected node (T2) linked with four Tb^{3+} ions (T1). (c) Zeolite-like topology given through the four-connected nodes (Tb, green; phenyl group, gray). (d) Eight-membered ring consisting of four metal centers and four phenyl groups linked through carboxylic groups. (e) Approximately 13 Å × 7 Å rectangle channels viewed down the [1,1,0] direction.

via emission of visible radiation named as luminescence.[13] In this paper, we investigated the luminescence properties of these complexes. The solid-state photoluminesecent spectra of complex **1** and free H_3BTC at room temperature are given in Figure 3. As can be seen, there are two emission groups for complex **1** in the ranges of 350−450 nm (λ_{ex} = 235 nm; Figure 3a) and 450−650 nm (λ_{ex} = 254 nm; Figure 3b). The emission ranging from 450 to 650 nm is attributed to the typical peaks of the Tb^{3+} ion, which occur from $^5D_4$ to ^7F_J (J = 6, 5, 4, 3) correspondingly.[14] Compared with free H_3BTC, complex **1** exhibits two red-shifted emission bands and one main peak without any shift in the range of 350−450 nm. The red-shifted emission bands from 380 to 450 nm are probably related to the intraligand fluorescent emission; a similar red-shifted emission had been observed previously.[15] The main emission peak (387 nm) of compound **1** and free H_3BTC may be attributed to $\pi^* \rightarrow$ n.[16] In the range of 350−450 nm (λ_{ex} = 235 nm), complexes **2**, **4**, and **5** have red-shifted peaks similar to that of complex **1** and an additional blue shift, which would be assigned to the emission of the ligand-to-metal charge transfer[17] (Figure S1 in the Supporting Information).

Magnetic Properties. The temperature-dependent magnetic susceptibility data of complexes **1**−**5** have been measured for polycrystalline samples at an applied magnetic field of 1000 Oe in the temperature range of 4−300 K. For complex **1** (Figure 4), the observed value of $\chi_M T$ per [Tb] unit is 10.70 $cm^3 \cdot K \cdot mol^{-1}$ at room temperature, which is slightly smaller than the value, 11.82 $cm^3 \cdot K \cdot mol^{-1}$, of a free Tb^{3+} ion in the $^7F_6$ state.[18] Also, with a decrease of temperature, the value of $\chi_M T$ decreases. The plot of $\chi_M{}^{-1}$ vs T over the whole temperature range obeys the Curie−Weiss law [$\chi = C/(T - \theta)$] with C = 10.87 $cm^3 \cdot K \cdot mol^{-1}$ and θ = −2.97 K. The decrease of $\chi_M T$ and the negative

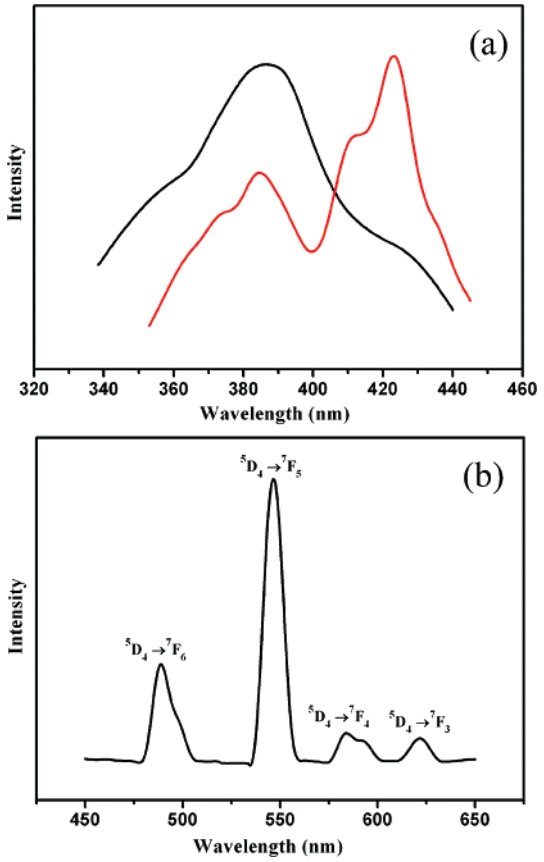

Figure 3. Photoluminesecent spectra of (a) complex **1** (red) and free H_3-BTC (black) excited at 235 nm and (b) complex **1** excited at 254 nm.

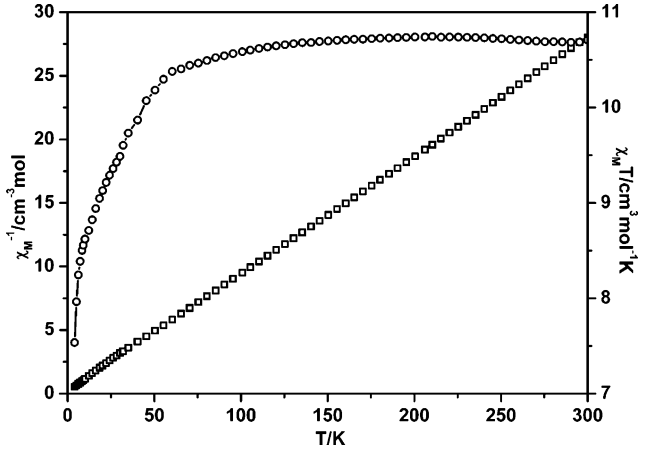

Figure 4. Plots of the temperature dependence of $\chi_M{}^{-1}$ (open squares) and $\chi_M T$ (open circles) for complex **1**.

(13) (a) Yan, B.; Zhang, H.; Wang, S.; Ni, J. *Mater. Res. Bull.* **1998**, *33*, 1517. (b) Zhang, H. J.; Yan, B.; Wang, S. B.; Ni, J. Z. *J. Photochem. Photobiol. A: Chem.* **1997**, *109*, 223. (c) Hong, X. L.; Li, Y. Z.; Hu, H. M.; Pan, Y.; Bai, J. F.; You, X. Z. *Cryst. Growth Des.* **2006**, *6*, 1223.
(14) Zhao, B.; Chen, X. Y.; Cheng, P.; Liao, D. Z.; Yan, S. P.; Jiang, Z. H. *J. Am. Chem. Soc.* **2004**, *126*, 15394.
(15) (a) Chen, W.; Wang, J. Y.; Chen, C.; Yue, Q.; Yuan, H. M.; Chen, J. S.; Wang, S. N. *Inorg. Chem.* **2003**, *42*, 944. (b) Thirumurugan, A.; Natarajan, S. *Dalton Trans.* **2004**, 2923.
(16) Thirumurugan, A.; Natarajan, S. *Dalton Trans.* **2004**, 2923.
(17) (a) Dai, J. C.; Wu, X. T.; Fu, Z. Y.; Cui, C. P.; Hu, S. M.; Du, W. X.; Wu, L. M.; Zhang, H. H.; Sun, R. Q. *Inorg. Chem.* **2002**, *41*, 1391. (b) Zhang, L. Y.; Liu, G. F.; Zheng, S. L.; Ye, B. H.; Zhang, X. M.; Chen, X. M. *Eur. J. Inorg. Chem.* **2003**, 2965.
(18) (a) Benelli, C.; Gatteschi, D. *Chem. Rev.* **2002**, *102*, 2369. (b) Zheng, X.; Wang, Z.; Gao, S.; Liao, F.; Yan, C.; Jin, L. *Eur. J. Inorg. Chem.* **2004**, 2968.

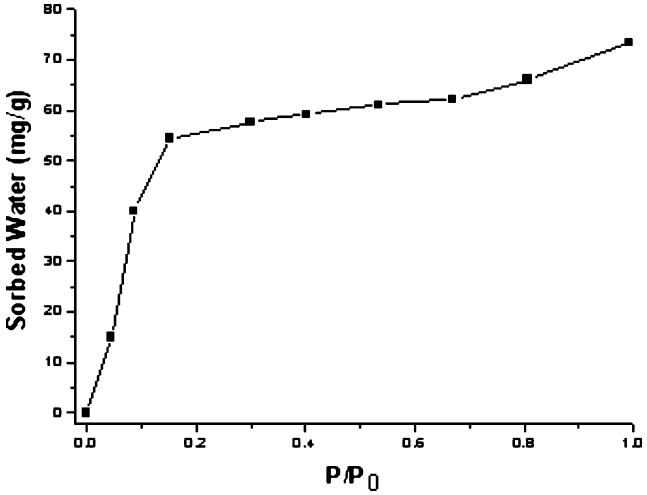

Figure 5. Water sorption spectrum of complex **4**.

value of θ indicate that the antiferromagnetic interaction between the Tb^{3+} ions dominates the magnetic properties of complex **1**. All of complexes **2**−**5** have $\chi_M T$ vs T plots similar to that of complex **1** and negative values of θ, so this series of complexes exhibit similar antiferromagnetic interactions between Ln^{3+} ions (Figure S2 in the Supporting Information).

Thermal Stability and Water Sorption Properties. The thermal stability of complex **4** has been studied through TGA, which was performed from 35 to 800 °C. The first weight loss of 31.49% from 35 to 250 °C corresponds to a loss of one guest water molecule and one coordinated DMF molecule (calcd: 30.49%). The decomposition of complex **4** starts above 375 °C, and the remaining weight of 34.07% corresponds to the percentage of the erbium and oxygen components, Er_2O_3 (calcd: 35.51%) (Figure S3 in the Supporting Information). The water adsorption isotherm for complex **4** was also measured at room temperature (Figure 5). The sample of complex **4** was evacuated under reduced pressure (1×10^{-5} Torr) until there was no more weight loss and then exposed to a water vapor sorbate. Type I behavior in the range $P/P_0 = 0-0.7$ was observed, which clearly indicated that incoming guests could move into the channels and the frameworks could maintain the porosity throughout the process. The second augment of the amounts adsorbed in the range $P/P_0 > 0.7$ can be attributed to adsorption on an external crystalline surface.[19] At $P/P_0 = 0.7$, the amounts of complex **4** adsorbed were 65 for water, which are equivalent to about 15 water molecules per unit cell that can be adsorbed into the micropores of dehydrated complex **4**.

(19) Eddaoudi, M.; Li, H. L.; Yaghi, O. M. *J. Am. Chem. Soc.* **2000**, *122*, 1391.

IR Spectrum. These complexes display similar IR spectra (Figure S4 in the Supporting Information). The asymmetric and symmetric stretching vibrations of the carboxylate groups have bands at 1555 and 1383 cm^{-1}. The bands at 1620, 3077, 690, and 780 cm^{-1} are attributed to the aromatic skeleton vibration of the benzene ring, $\nu_{=CH}$ of benzene, $\delta_{=CH}$ out of the face of benzene, and the 1,4-substituents of the benzene ring, respectively. The bands at 1677 and 2916 cm^{-1} are from $\nu_{=CO}$ and the asymmetric stretching vibration of the methyl group of the DMF molecules. The lack of IR bands at 2657, 2545 (OCOOH), and 1690 (CCOOH) cm^{-1} indicates the complete deprotonation of H_3BTC after the reaction. The broad band centered at 3430 cm^{-1} is attributed to the hydrogen-bonded ν_{OH} groups mainly from adsorbed water.[20]

Conclusions

A series of lanthanide MOFs with zeolite-like topology have been synthesized and exhibit the same 3D open framework with approximate 13 Å × 7 Å rectangle eight-membered ring channels along the [1,1,0] and [1,−1,0] directions, respectively. The structure contains inorganic four-conneced nodes (T1, Ln^{3+} ions) and organic four-connected nodes (T2, phenyl groups), and both of the vertex symbols of the four-connected nodes (T1 and T2) are 4·4·4·6·6·8, which is very common in zeolite topologies. These complexes exhibit predominant fluorescence in the visible region, and complex **1** shows a Tb^{3+} characteristic emission in the range of 450−650 nm. The antiferromagnetic interaction between Ln^{3+} ions is observed in complexes **1**−**5**. The water sorption isotherm reveals that 15 water molecules per unit cell can be adsorbed into the micropores. Thus, these could be anticipated as potential fluorescent and magnetic porous materials.

Acknowledgment. This research was supported by the State Basic Research Project (2006CB806100), Outstanding Young Scientist Foundation of NSFC (20625102), NSFC (Grant nos. 20571030, 20531030, and 20371020), "111" Project of Ministry of Education and Science and Technology Office of Jilin Province.

Supporting Information Available: TGA, the magnetic behavior of complexes **2**−**5**, IR spectra, XRD patterns, and crystal data in CIF format. This material is available free of charge via the Internet at http://pubs.acs.org.

IC061666I

(20) (a) Fang, Q. R.; Shi, X.; Wu, G.; Tian, G.; Zhu, G. S.; Wang, R. W.; Qiu, S. L. *J. Solid State Chem.* **2003**, *176*, 1. (b) Tian, G.; Zhu, G. S.; Yang, X. Y.; Fang, Q. R.; Xue, M.; Sun, J. Y.; Wei, Y.; Qiu, S. L. *Chem. Commun.* **2005**, 1396.